Supplementary material for Metal-Water Interface Formation: Thermodynamics from Ab-Initio Molecular Dynamics Simulations

Fabiola Domínguez-Flores,[†] Toni Kiljunen,[‡] Axel Groß,[†] Sung Sakong,[*,†] and Marko M. Melander[*,‡]

[†]*Institute of Theoretical Chemistry, Ulm University, 89069 Ulm, Germany*

[‡]*Nanoscience Center, Department of Chemistry, University of Jyväskylä, P.O. Box 35 (YN), FI-40014 Jyväskylä, Finland*

E-mail: sung.sakong@uni-ulm.de; marko.m.melander@jyu.fi

Details on the free energy calculations

The interfacial thermodynamic quantities reported in the main manuscript were computed by following the thermodynamic cycle in Figure 1. In particular, the following quantities and definitions were used in computing the needed free energies, internal energies, and entropies.

1. The free energies of the main target interface F_{sl}, and the reference systems (bulk water F_{l}, bulk solids F_{s}, water film F_{lv}, and bare metal surfaces F_{sv}), were obtained from the time-averaged internal energies and entropies using the DFT-MD trajectories and following the 2PT analysis (see Numerical methods in the main manuscript).

2. The free energy of forming the liquid–vacuum interface was calculated from the water film configuration and assigning the vacuum energy to zero. The free energy of formation of the water–vacuum interface was defined as

$$\Delta F_{\mathrm{lv}} = F_{\mathrm{lv}} - F_{\mathrm{l}} \tag{S1}$$

and the corresponding surface tension was calculated as

$$\gamma_{\mathrm{lv}} = \frac{1}{2A_{\mathrm{lv}}} \Delta F_{\mathrm{lv}} \,, \tag{S2}$$

where $2A_{\mathrm{lv}}$ is the total area of the two-sided water film. The resulting $\gamma_{\mathrm{lv}} = 4.46$ meV Å^{-2} (0.715 N m^{-1}) is in a good agreement with the literature value of 0.728 N m^{-1}.[1]

3. The surface solvation energy F_{solv} was computed using the same number of metal atoms (180) for the target interface sl as for the separated metal–vacuum (sv) system. To reference against the bulk liquid, the surface tension γ_{lv} due to the presence of a liquid–vacuum interface in the metal–water model, was subtracted from F_{solv}. The solvation energy was thereby calculated as

$$F_{\mathrm{solv}} = \frac{1}{A_{\mathrm{sl}}} \left[F_{\mathrm{sl}} - F_{\mathrm{sv}} - 144(F_{\mathrm{l}}/96) - \gamma_{\mathrm{lv}} A_{\mathrm{sl}} \right] , \tag{S3}$$

where A_{sl} is the area of the studied solid–liquid interface and the number of water molecules match those used in the actual MD simulations. Since the bottom two atomic layers were frozen to their bulk positions in both sl and sv trajectories, we assumed that their contributions to the total energy cancel out.

4. When referencing the F_{sl} against the bulk solid, also the contribution of solid–vacuum interface formation and corresponding sv surface tension was subtracted from ΔF_{sl}. To this end, we defined two surface tensions in the sv model: γ_{sv} for the mobile top surface and $\bar{\gamma}_{\mathrm{sv}}$ for the immobile bottom surface. The surface tension $\bar{\gamma}_{\mathrm{sv}}$ thus originates from a fixed metal slab of the same 180-atom size as the one used for the F_{sv}, whereas the fixed bulk version of the

s system was modelled as a single atom in the bulk unit cell. Because the atomic positions were kept fixed in these auxiliary reference models for sv and s, the entropy contributions vanish and only the internal energies $\bar{E}$ of the fixed system contribute to the free energy. The surface tension due to the fixed side of the slab becomes

$$\bar{\gamma}_{\mathrm{sv}} = \frac{1}{2A_{\mathrm{sv}}} \left[\bar{E}_{\mathrm{sv}} - 180(\bar{E}_{\mathrm{s}}/216)\right] . \tag{S4}$$

The total surface tension was approximated as the average $\gamma_{\mathrm{sv,tot}} = (\gamma_{\mathrm{sv}} + \bar{\gamma}_{\mathrm{sv}})/2$ so that the contribution from the mobile-side was calculated as

$$\gamma_{\mathrm{sv}} = \frac{1}{A_{\mathrm{sv}}} \left[F_{\mathrm{sv}} - 108(F_{\mathrm{s}}/216) - 72(\bar{E}_{\mathrm{s}}/216)\right] - \bar{\gamma}_{\mathrm{sv}} . \tag{S5}$$

Taking the numbers of atoms and molecules explicitly into account (108 mobile and 72 frozen atoms in slab, 216 atoms in bulk metal, 144 water molecules in the film and 96 in the bulk model), the free energy of formation of the metal–water interface becomes

$$\Delta F_{\mathrm{sl}} = F_{\mathrm{sl}} - \left[144(F_{\mathrm{l}}/96) + \gamma_{\mathrm{lv}} A_{\mathrm{sl}}\right] - \left[108(F_{\mathrm{s}}/216) + 72(\bar{E}_{\mathrm{s}}/216) + \bar{\gamma}_{\mathrm{sv}} A_{\mathrm{sl}}\right] \tag{S6}$$

as can be seen from black arrows of the thermodynamic cycle in Figure 1. The surface tension of the sl interface was then calculated as

$$\gamma_{\mathrm{sl}} = \frac{\Delta F_{\mathrm{sl}}}{A_{\mathrm{sl}}} . \tag{S7}$$

5. After the (free) energies were calculated and the (free) energies of the surface formation were obtained, we also computed the experimentally accessible work of adhesion W_{ad}. The work of adhesion amounts to the energy of separation of the sl interface into the sv and lv

components per unit area, which can be written as

$$\begin{aligned} W_{\mathrm{ad}} &= \frac{F_{\mathrm{lv}} + F_{\mathrm{sv}} - F_{\mathrm{sl}}}{A_{\mathrm{sl}}} \\ &= \frac{F_{\mathrm{l}} + \gamma_{\mathrm{lv}} A_{\mathrm{sl}} + F_{\mathrm{s}} + \gamma_{\mathrm{sv}} A_{\mathrm{sl}} - (F_{\mathrm{l}} + F_{\mathrm{s}} + \gamma_{\mathrm{sl}} A_{\mathrm{sl}})}{A_{\mathrm{sl}}} \\ &= \gamma_{\mathrm{lv}} + \gamma_{\mathrm{sv}} - \gamma_{\mathrm{sl}} \,. \end{aligned} \tag{S8}$$

The bulk terms cancel out and the number of species remains constant.

6. W_{ad} can also be obtained from the solid–liquid contact angle θ_{sl} through the Young–Dupré equation:

$$\cos(\theta_{\mathrm{sl}}) = \frac{W_{\mathrm{ad}}}{\gamma_{\mathrm{lv}}} - 1 \,. \tag{S9}$$

We used this equation to obtain the contact angle using the computed adhesion work and γ_{lv}. Note, that the contact angle is zero whenever $W_{\mathrm{ad}} > 9.1$ meV/Å^2. This limits the usability of contact angle measurements as has been reported before.[2,3]

Computation of Interfacial Entropies

As discussed in the main manuscript Section "Analyzing interfacial metal-water thermodynamics", we studied the interfacial entropy by separating the water film on the metal surface to 1WL and IBL contributions. These definitions are based on the distance of the water molecules from the metal surface as discussed in "Analyzing the interfacial structure and entropy" section. Because the water molecules constituting the 1WL and IBL regions cannot be ambiguously defined due to the movement of molecules between these regions, we studied how the interfacial entropy depends on the assignment of molecules to these regions. For this we used the residence time to quantify how many water molecules stay in the 1WL and IBL regions and compare the results in Table S1. The residence time 100 % corresponds to the case where only those water molecules that stay in the 1WL for the entire duration of the simulation are considered to constitute the 1WL subset. Accordingly, 80 % and 50 % correspond to cases where the water molecules spend 80 % and 50 % of the simulation time in the 1WL. Zero corresponds to the case where all molecules that visit 1WL at least once during the simulation are considered to be a part of the 1WL. The comparison in Table SI1 shows that while the absolute interfacial entropies and number of water molecules at 1WL differ depending on the used residence time, the overall trends are robust enough for the qualitative discussion in the main manuscript.

With Rh(111) surface, the DFT-MD production run exhibited a splitting of water molecule already in the beginning, as we found one hydroxyl ion and one hydronium in the trajectory. The setup for the DoSPT code allows to specify these species in the so called supergroups file. In order to track the identity, formation, and annihilation of the split species, the topology file was also created. Therefore, the difference of number of molecules established in the supergroups file at the start of the simulation and at the end of the trajectory can be obtained from the DoSPT code, but since the entropy of a single particle is not accurate or thermodynamically meaningful, we report only results that do not require to account for water splitting.

Table S1: Interfacial entropies of water on metal surfaces (meV per molecule at $T = 298$ K) using the residence time analysis

Residence time (%)	100	80	50	0
		Au(111)		
n (1WL)	6	23	24	29
$\langle S \rangle T$ (1WL)	256	225	224	218
$\langle S \rangle T$ (IBL)	205	197	191	190
		Ag(111)		
n (1WL)	4	20	24	29
$\langle S \rangle T$ (1WL)	270	230	225	219
$\langle S \rangle T$ (IBL)	201	190	187	187
		Pt(111)		
n (1WL)	16	22	25	27
$\langle S \rangle T$ (1WL)	181	177	176	175
$\langle S \rangle T$ (IBL)	189	182	179	182
		Pd(111)		
n (1WL)	11	20	24	27
$\langle S \rangle T$ (1WL)	236	202	184	236
$\langle S \rangle T$ (IBL)	178	199	195	200
		PdAu(111)		
n (1WL)	13	22	26	28
$\langle S \rangle T$ (1WL)	166	166	167	170
$\langle S \rangle T$ (IBL)	204	204	192	186
		Rh(111)		
n (1WL)	9	18	21	27
$\langle S \rangle T$ (1WL)	211	210	195	70
$\langle S \rangle T$ (IBL)	196	172	189	126

The bending and stretching mode DoS for interfacial and bulk water

The bending and stretching modes lead to a sharp Lorentzian peak around 1600 cm^{-1} and a skewed Gaussian around 3000 to 3600 cm^{-1}, respectively.

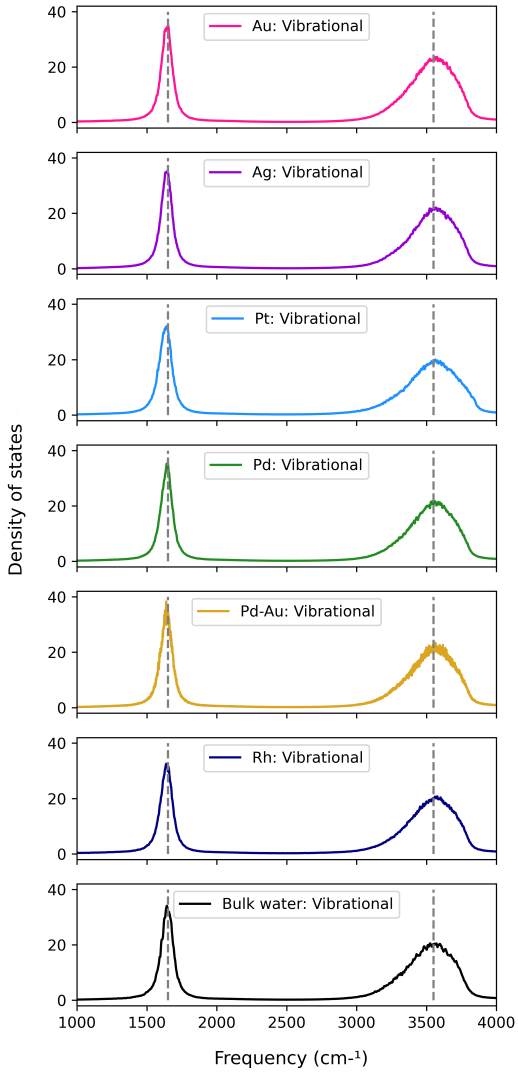

Figure S1: Comparison of the water vibrational DoS on Au(111), Ag(111), Pt(111), Pd(111), Pd-Au(111), and Rh(111) to bulk water. The dashed lines show the bending (left) and stretching (right) mode intensity maxima in bulk water.

Electrostatic potential profiles

To analyze the DFT-produced electrostatic potentials, we employed the Density Derived Electrostatic and Chemical approach (DDEC), which uses a specific charge partitioning scheme to define the net atomic charge for each atom.[4,5] To present the ESP profiles at the interfaces, we summed the net atomic charges in the metal slab and determined the charge transfer from the water film to the metal electrode.

The electrostatic potential profile of the metal–water interfaces is presented in Figure S2. We note that the electrostatic potentials in the bulk water region on all the considered metal electrodes except Rh are aligned with respect to the vacuum level. Due to the charge transfer and the water splitting, the water film on Rh is positively polarized and shows a lower bulk level than the other metals. Rh and Pd have the highest fluctuations within the 1WL but Rh features a small shoulder due to the adsorbed water layer (Figure 3) and the accompanying charge transfer between Rh and water. The electrostatic profile of Au and Ag exhibit smaller fluctuations within the 1WL and are very similar. Fluctuations in the electrostatic potential become less pronounced when moving away from the surface, and fluctuations are largest for the most strongly binding surfaces, Rh and Pt.

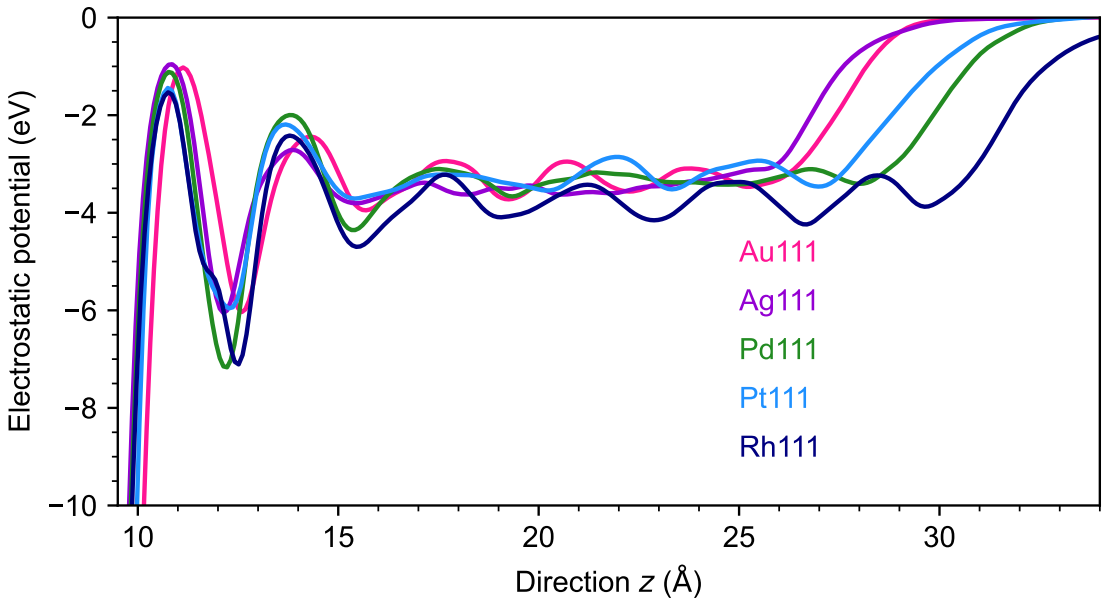

Figure S2: Electrostatic potential profiles for the metal–water interfaces as function of distance from the metal surface.

References

(1) Zhang, Y.; Feller, S. E.; Brooks, B. R.; Pastor, R. W. Computer simulation of liquid/liquid interfaces. I. Theory and application to octane/water. *The Journal of Chemical Physics* **1995**, *103*, 10252–10266.

(2) Bewig, K. W.; Zisman, W. A. The Wetting of Gold and Platinum by Water. *The Journal of Physical Chemistry* **1965**, *69*, 4238–4242.

(3) Schrader, M. E. Ultrahigh-vacuum techniques in the measurement of contact angles. II. Water on gold. *The Journal of Physical Chemistry* **1970**, *74*, 2313–2317.

(4) Manz, T. A.; Limas, N. G. Introducing DDEC6 atomic population analysis: part 1. Charge partitioning theory and methodology. *RSC Adv.* **2016**, *6*, 47771–47801.

(5) Limas, N. G.; Manz, T. A. Introducing DDEC6 atomic population analysis: part 2. Computed

results for a wide range of periodic and nonperiodic materials. *RSC Adv.* **2016**, *6*, 45727–45747.